

Generation of coherence via Gaussian measurements

Francesco Albarelli* and Marco G. Genoni†

Quantum Technology Lab, Dipartimento di Fisica, Università degli Studi di Milano, 20133 Milano, Italy

Matteo G. A. Paris‡

*Quantum Technology Lab, Dipartimento di Fisica, Università degli Studi di Milano, 20133 Milano, Italy
and INFN, Sezione di Milano, I-20133 Milano, Italy*

(Received 15 May 2017; published 31 July 2017)

We address measurement-based generation of quantum coherence in continuous variable systems. We consider Gaussian measurements performed on Gaussian states and focus on two scenarios: In the first one, we assume an initially correlated bipartite state shared by two parties and study how correlations may be exploited to remotely create quantum coherence via measurement back action. In particular, we focus on conditional states with zero first moments, so as to address coherence due to properties of the covariance matrix. We consider different classes of bipartite states with incoherent marginals and show that the larger the *measurement squeezing*, the larger the conditional coherence. Homodyne detection is thus the optimal Gaussian measurement to remotely generate coherence. We also show that for squeezed thermal states there exists a threshold value for the generated coherence which separates entangled and separable states at a fixed energy. Finally, we briefly discuss the tripartite case and the relationship between tripartite correlations and the conditional two-mode coherence. In the second scenario, we address the steady-state coherence of a system interacting with an environment which is continuously monitored. In particular, we discuss the dynamics of an optical parametric oscillator in order to investigate how the coherence of a Gaussian state may be increased by means of time-continuous Gaussian measurement on the interacting environment.

DOI: [10.1103/PhysRevA.96.012337](https://doi.org/10.1103/PhysRevA.96.012337)

I. INTRODUCTION

Coherence is the main ingredient for the observation of interference, a physical phenomenon at the basis of several applications in science and technology. In addition, since the superposition principle is the main point of departure from classical physics, coherence is also at the basis of purely quantum features, such as entanglement, and it plays a pivotal role in the description of quantum states and operations. In turn, coherence is a key concept in several fields, ranging from quantum optics [1–3] to quantum information [4,5], quantum thermodynamics [6,7], and quantum estimation [8], as well as in several phenomena in biological systems [9].

Even if quantum coherence has long been recognized as a resource in many contexts, a systematic study from a resource-theoretical point of view has started only recently [10] and it is undergoing very active development (see [11] for a recent review). In turn, the generation and manipulation of coherence in bipartite and multipartite systems, as well as the interplay with quantum correlations, are topics which have recently gained considerable attention [12–19]. Our aim here is to explore these connections in continuous variable systems and, in particular, for Gaussian states and operations. As a matter of fact, despite quantum coherence having been discussed mostly for finite-dimensional systems, a resource-theoretic framework for coherence for infinite-dimensional Fock space has been introduced [20] and the coherence of Gaussian states has been studied in some detail

[21,22]. We also mention that for continuous variable systems, coherence in the nonorthogonal coherent states basis has recently been investigated [23–25] and linked to P function nonclassicality.

In this paper, we address the issue of generating quantum coherence in the Fock basis by performing Gaussian measurements on Gaussian states. We analyze two scenarios in detail. In the first case, we assume an initially correlated bipartite state shared by two distant laboratories. The two marginal states are initially incoherent and we analyze how correlations can be exploited to remotely create quantum coherence via measurement back action. In the second case, we study the coherence of the steady state of a system interacting with an environment which is continuously monitored, i.e., subject to continuous-time Gaussian measurements. Also in this case, correlations between the environment and the system, which are provided by the dynamics, play a role in the generation of coherence. In order to address only the coherence due to the covariance matrix (CM), i.e., to correlations, most of the results are obtained neglecting the first moments. However, for the sake of completeness, some results including first moments are reported in the Appendix.

The paper is structured as follows. In Sec. II we briefly recall the formalism for bosonic Gaussian states and operations and set the notation. In Sec. III, we review coherence measures which are suitable for Gaussian states also highlighting some connections between quantum correlations and quantum coherence. Section IV is devoted to the (conditional) remote creation of quantum coherence starting either from generic two-mode Gaussian states in normal form or from a specific class of three-mode states. Section V deals with coherence enhancement due to continuous measurements on the environmental modes. In particular, we focus on the example of

*francesco.albarelli@unimi.it; <http://users.unimi.it/aqm>

†marco.genoni@fisica.unimi.it; <http://users.unimi.it/aqm>

‡matteo.paris@fisica.unimi.it; <http://users.unimi.it/aqm>

a monitored parametric oscillator. Finally, Sec. VI closes the paper with some concluding remarks.

II. GAUSSIAN STATES AND MEASUREMENTS

We consider a set of n bosonic modes described by a vector of quadrature operators $\hat{\mathbf{r}}^\top = (\hat{x}_1, \hat{p}_1, \dots, \hat{x}_n, \hat{p}_n)$ that satisfy the canonical commutation relation $[\hat{r}_j, \hat{r}_k] = i\Omega_{jk}$, where Ω is the symplectic matrix

$$\Omega = \bigoplus_{j=1}^n \omega, \quad \text{with} \quad \omega = \begin{pmatrix} 0 & 1 \\ -1 & 0 \end{pmatrix}. \quad (1)$$

A quantum state ϱ is defined as Gaussian if and only if it can be written as a ground or thermal state of a quadratic Hamiltonian, i.e.,

$$\varrho = \frac{\exp\{-\beta\hat{\mathcal{H}}_G\}}{\mathcal{Z}}, \quad \beta \in \mathbb{R}, \quad (2)$$

where $\hat{\mathcal{H}}_G = \hat{\mathbf{r}}^\top H_G \hat{\mathbf{r}}/2$ and $H_G \geq 0$ [26]. Gaussian states can be univocally described by the vector of first moments $\bar{\mathbf{r}}$ and the covariance matrix σ :

$$\bar{\mathbf{r}} = \text{Tr}[\varrho\hat{\mathbf{r}}], \quad \sigma_{ij} = \text{Tr}[\varrho\{(\hat{r}_i - \bar{r}_i)(\hat{r}_j - \bar{r}_j)^\top\}]. \quad (3)$$

In order to describe a proper Gaussian quantum state, the CM has to satisfy the physicality condition [27]:

$$\sigma + i\Omega \geq 0. \quad (4)$$

A generic bipartite Gaussian state is completely described by a first-moment vector and a block-form CM,

$$\bar{\mathbf{r}} = \begin{pmatrix} \bar{\mathbf{r}}_A \\ \bar{\mathbf{r}}_B \end{pmatrix}, \quad \sigma = \begin{pmatrix} \sigma_A & \sigma_{AB} \\ \sigma_{AB} & \sigma_B \end{pmatrix}, \quad (5)$$

where $\bar{\mathbf{r}}_A$, σ_A and $\bar{\mathbf{r}}_B$, σ_B are the first moments and covariance matrices of the marginal states, while σ_{AB} contains the correlations between the two subsystems. A necessary and sufficient condition for the entanglement of a bipartite Gaussian state has been derived in [28], by applying the physicality condition, (4), to the CM of the partially transposed state.

In this paper, we deal with Gaussian measurements on bipartite Gaussian states. A generic Gaussian measurement is described by a probability operator-valued measure (POVM) of the form $\Pi(\mathbf{r}) = D(\mathbf{r})\varrho_G D^\dagger(\mathbf{r})$, where ϱ_G is a Gaussian state and $D(\mathbf{r})$ is the displacement operator. Any Gaussian measurement is thus naturally associated with the covariance matrix σ_m of a Gaussian state, and in particular, measurements involving ideal detectors with no losses correspond to pure states such that $\det \sigma_m = 1$. Gaussian measurements include the case of homodyne and heterodyne detections, whose CMs for single-mode detection read

$$\sigma_m^{(\text{hom})} = \lim_{s \rightarrow 0} R(\phi) \begin{pmatrix} s & 0 \\ 0 & s^{-1} \end{pmatrix} R^\top(\phi), \quad \sigma_m^{(\text{het})} = \mathbb{1}_2, \quad (6)$$

respectively, where $R(\phi)$ denotes a real rotation matrix.

Given an initial bipartite Gaussian state, with moments given in (5), the conditional state for subsystem A after a Gaussian measurement σ_m on subsystem B , has the covariance

matrix and first-moments vector [26,29]

$$\begin{aligned} \sigma'_A &= \sigma_A - \sigma_{AB}(\sigma_B + \sigma_m)^{-1}\sigma_{AB}^\top, \\ \mathbf{r}'_A &= \mathbf{r}_A + \sigma_{AB}(\sigma_B + \sigma_m)^{-1}(\mathbf{r}_{\text{out}} - \mathbf{r}_B), \end{aligned} \quad (7)$$

where the vector \mathbf{r}_{out} is the vector of the outcomes, which are distributed according to a Gaussian centered at \mathbf{r}_B :

$$p(\mathbf{r}_{\text{out}}) = \frac{e^{-(\mathbf{r}_{\text{out}} - \mathbf{r}_B)^\top (\sigma_m + \sigma_B)^{-1} (\mathbf{r}_{\text{out}} - \mathbf{r}_B)}}{\pi \sqrt{\det(\sigma_m + \sigma_B)}}. \quad (8)$$

III. COHERENCE MEASURES FOR GAUSSIAN STATES

A. Resource theory of coherence in the Fock space

We consider the infinite-dimensional Hilbert space of a single-mode bosonic system and the Fock basis $\{|n\rangle\}_{n=0}^\infty$ as the reference basis to assess the coherence of a state. The Fock states are defined as the eigenstates $H|n\rangle = n|n\rangle$ of the harmonic oscillator free Hamiltonian $H = \frac{1}{2}(\hat{x}^2 + \hat{p}^2 - 1)$. This is the most natural choice for discussing quantum coherence of bosonic continuous variable states [20–22].

We denote by \mathcal{I} the set of incoherent states $\delta = \sum_n \delta_n |n\rangle\langle n|$ with $\sum_n \delta_n = 1$, where all the sums run from 0 to ∞ . Incoherent quantum operations ϕ_{ICPTP} [10] are completely positive and trace-preserving (ICPTP) maps $\phi_{\text{ICPTP}}(\circ) = \sum_n K_n \circ K_n^\dagger$, $\sum_n K_n K_n^\dagger = \mathbb{1}$ for which $K_n \mathcal{I} K_n^\dagger \subset \mathcal{I}$, i.e., the Kraus operators of ICPTP maps send incoherent states to incoherent states. This is the resource theoretical framework we use throughout the paper. Note that different definitions of incoherent operations may be employed, which leads to different resource theories [30–32].

Any coherence measure functional C should satisfy the following properties.

(C1) $C(\rho) \geq 0 \forall \rho$ with $C(\rho) = 0 \Leftrightarrow \rho \in \mathcal{I}$;

(C2a) monotonicity under ICPTP operations, $C(\rho) \geq C(\phi_{\text{ICPTP}}(\rho))$;

(C2b) monotonicity under selective measurements, on average, $C(\rho) \geq \sum_n p_n C(\rho_n) \quad \forall K_n$, with $\rho_n = K_n \rho K_n^\dagger / p_n$ and $p_n = \text{Tr}[K_n \rho K_n^\dagger]$;

(C3) convexity, i.e., C is nonincreasing under mixing, $\sum p_n C(\rho_n) \geq C(\sum p_n \rho_n)$.

Furthermore, for states of an infinite-dimensional system, we require that states with finite energy (i.e., a finite average number of bosonic excitations) have a finite coherence [20]:

(C4) $\text{Tr}[\rho \hat{n}] < \infty \Rightarrow C(\rho) < \infty$.

We point out that requirements (C2b) and (C3) are equivalent to the additivity of coherence for block diagonal density operators in the reference basis [33].

A class of coherence measures is then obtained by minimizing any pseudodistance of the quantum state under investigation from the set of incoherent states \mathcal{I} . A convenient choice is given by the quantum relative entropy $S(\rho||\sigma) = -\text{Tr}[\rho \log_2 \sigma] - S(\rho)$, where $S(\rho) = -\text{Tr}[\rho \log_2 \rho]$ is the Von Neumann entropy of the density matrix ρ . The resulting measure is the so-called relative entropy of coherence

$$C_S = \min_{\delta \in \mathcal{I}} S(\rho||\delta) = S(\rho||\rho_{\text{diag}}) = S(\rho_{\text{diag}}) - S(\rho), \quad (9)$$

where ρ_{diag} is the original state with all the off-diagonal elements in the reference basis suppressed. This measure

satisfies all properties (C1)–(C3) and, crucially, also property (C4) [20]. As a consequence, it is a good coherence monotone for infinite-dimensional systems.

The explicit expression of the relative entropy of coherence in the Fock basis is given by

$$C_S(\rho) = H(\{p_n\}) - S(\rho), \quad (10)$$

where $\{p_n = \langle n|\rho|n\rangle\}$ is the photon number distribution and $H(\{p_n\}) = -\sum_{i=0}^{\infty} p_n \log_2(p_n)$ is the classical Shannon entropy. This expression has the drawback that $H(\{p_n\})$ is not easy to obtain in closed form even in the case of Gaussian states. We also note that the relative entropy of coherence may also be expressed in terms of the entropic measure of non-Gaussianity $\delta(\rho)$ [34,35] as

$$C_S(\rho) = \delta(\rho) + H(\{p_n\}) - h(\sqrt{\det \sigma}), \quad (11)$$

where σ is the CM of ρ and $h(x) = (x + \frac{1}{2}) \ln(x + \frac{1}{2}) - (x - \frac{1}{2}) \ln(x - \frac{1}{2})$.

The relative entropy of coherence can be straightforwardly extended to multimode Fock space [20]; for example, for a two-mode state it reads

$$C_S(\rho_{AB}) = H(\{p_{nm}\}) - S(\rho_{AB}), \quad (12)$$

with $p_{nm} = \langle n,m|\rho_{AB}|n,m\rangle$.

B. Gaussian coherence

The resource theory of coherence has also been studied focusing on Gaussian states. In this case one is interested in ICPTP operations which preserve the Gaussian character of the state [21]. For single-mode systems the set of incoherent Gaussian states \mathcal{I}_G only includes thermal states [21,22] (which we label with the Greek letter ν). For multimode systems, the only incoherent states are locally thermal states (tensor products of thermal states), i.e., $\otimes_{i=1}^m \nu_i$ for an m -mode state [21], whose covariance matrix is a direct sum of multiple identity matrices $\sigma_\nu = \oplus_{i=1}^m k_i \mathbb{1}_2$.

The Gaussian relative entropy of coherence is thus obtained by restricting the minimization to the set of incoherent Gaussian states \mathcal{I}_G [21]:

$$C_S^G(\rho_G) = \inf_{\nu \in \mathcal{I}_G} \{S(\rho_G||\nu) | \nu \in \mathcal{I}_G\}. \quad (13)$$

This is an upper bound to the relative entropy of coherence, as the closest incoherent state need not be Gaussian. For a single mode the closest Gaussian incoherent state is a thermal state with the same mean photon number, leading to

$$\begin{aligned} C_S^G(\rho_G) &= \min_{\nu \in \mathcal{I}_G} S(\rho_G||\nu) \\ &= S(\rho_G||\bar{\nu}) = S(\bar{\nu}) - S(\rho_G) \end{aligned} \quad (14)$$

$$= h(2\bar{n} + 1) - h(\sqrt{\det \sigma}) \quad (15)$$

$$= h\left(\frac{1}{2}\text{Tr}[\sigma] + |\mathbf{r}|^2\right) - h(\sqrt{\det \sigma}), \quad (16)$$

where $\bar{\nu}$ is the thermal state with $\bar{n} = \text{Tr}[\hat{n} \rho_G] = \frac{1}{4}\text{Tr}[\sigma] + \frac{1}{2}|\mathbf{r}|^2 - \frac{1}{2}$ thermal photons, and σ and \mathbf{r} are the covariance matrix and first-moment vector of the Gaussian state ρ_G . Expression (15) follows from Eq. (11) upon noting that for Gaussian states $\delta(\rho) \rightarrow 0$ and $H(\{p_n\}) \rightarrow H(\{\nu_n\}) \equiv$

$h(2\bar{n} + 1)$. Also, the Gaussian coherence may be generalized to m modes as

$$C_S^G(\rho_G) = \sum_{i=1}^m S(\bar{\nu}_i) - S(\rho_G), \quad (17)$$

where the $\bar{\nu}_i$ are single-mode thermal states at the energy of the i th mode, i.e., $\bar{n}_i = \frac{1}{4}(\text{Tr}[\sigma_i] + 2|\mathbf{r}_i|^2 - 2)$. Coherence measures based on proper geometrical distances, such as Bures and Hellinger distances, have also been investigated [22]. In the present work we focus on measures based on the relative entropy.

C. Coherence and correlations

There are tight relationships between quantum coherence and correlations [12,17,36–39]. Here we review and highlight some of these connections for bipartite Gaussian states. In a bipartite system with two local reference bases $\{|n\rangle_A\}$ and $\{|n\rangle_B\}$, the key quantity is the difference ΔC between the total coherence of the tensor product $\{|n\rangle_A \otimes |m\rangle_B\}$ and the local coherences. This quantity is also known as the correlated coherence [38,39]. Using the entropic measure of coherence C_S we have

$$\Delta C_S(\rho_{AB}) = C_S(\rho_{AB}) - [C_S(\rho_A) + C_S(\rho_B)] \quad (18)$$

$$\begin{aligned} &= H(\{p_{nm}\}) - S(\rho_{AB}) - H(\{p_n\}) - H(\{p_m\}) \\ &\quad + S(\rho_A) + S(\rho_B) \end{aligned} \quad (19)$$

$$= \mathcal{I}_q(\rho_{AB}) - \mathcal{I}(A : B); \quad (20)$$

i.e., ΔC_S is equal to the difference between the quantum mutual information $\mathcal{I}_q(\rho_{AB}) = S(\rho_A) + S(\rho_B) - S(\rho_{AB})$ and the classical mutual information $\mathcal{I}(A : B) = H(\{p_n\}) + H(\{p_m\}) - H(\{p_{nm}\})$ of a channel based on measurements in the reference basis.

The correlated coherence ΔC (independently of the coherence measure) has been introduced as a basis-independent measure of quantum correlations [38] by fixing the eigenbases of the marginal states as a reference so that $C_S(\rho_A) = C_S(\rho_B) = 0$. In particular, when the relative entropy of coherence is used, this measure corresponds to the measurement-induced disturbance [40], denoted $\mathcal{M}(\rho_{AB})$. From (18) we then have that the measurement-induced disturbance is an upper bound to the correlated coherence: $\Delta C_S(\rho_{AB}) \leq \mathcal{M}(\rho_{AB})$. Another measure of quantum correlations, the ameliorated measurement-induced disturbance, $\mathcal{A}(\rho_{AB})$, is obtained by minimizing the classical mutual information over all possible local POVMs. Crucially, the ameliorated measurement-induced disturbance is an upper bound to the (entropic) quantum discord $\mathcal{M}(\rho_{AB}) \geq \mathcal{A}(\rho_{AB}) \geq \max[D(A : B), D(B : A)] = M_D$, where $D(A : B)$ is the asymmetrical discord obtained by measuring subsystem B [41]. Given the minimization over all possible measurements in the definition of \mathcal{A} we have the following inequalities:

$$M_D \leq \mathcal{A}(\rho_{AB}) \leq \Delta C_S(\rho_{AB}) \leq C_S(\rho_{AB}). \quad (21)$$

We thus conclude that the relative entropy of coherence C_S on the tensor product of local bases of a bipartite system is an upper bound to the discord. This is in complete analogy with discrete variable systems [37], where the same results have

been obtained by resorting to a geometric measure of quantum discord.

Furthermore, if we consider the Gaussian relative entropy of coherence, then the quantity ΔC_S^G is equal to the quantum mutual information [42]:

$$\Delta C_S^G(\rho_{AB}) = C_S^G(\rho_{AB}) - (C_S^G(\rho_A) + C_S^G(\rho_B)) \quad (22)$$

$$= S(\bar{v}_A \otimes \bar{v}_B) - S(\rho_{AB}) - [S(\bar{v}_A) - S(\rho_A) + S(\bar{v}_B) - S(\rho_B)] \quad (23)$$

$$= S(\rho_A) + S(\rho_B) - S(\rho_{AB}) = \mathcal{I}_q(\rho_{AB}). \quad (24)$$

Overall, we obtain a further (loose) bound to the quantum discord in terms of Gaussian quantities, expressed by the chain of inequalities

$$M_D \leq \Delta C_S(\rho_{AB}) \leq \Delta C_S^G(\rho_{AB}) \leq C_S^G(\rho_{AB}). \quad (25)$$

IV. REMOTE CREATION OF COHERENCE

We now focus on the problem of remote creation of quantum coherence. In this scheme, we assume a correlated bipartite Gaussian state ρ_{AB} and we want to study the quantum coherence generated in subsystem A by performing Gaussian measurements on subsystem B . The term *remote* comes from the fact that the marginal states ρ_A and ρ_B , initially incoherent, may be manipulated at distant laboratories and one generates coherence in, say, system B by performing measurements on system A .

We first investigate the intuitive idea that performing *squeezed* measurements may induce coherence in an initially incoherent marginal state. The possibility of creating coherence is due to the subsystems' being correlated (not necessarily entangled). Therefore, we also study the interplay between the correlations and the remotely obtainable coherence. We show that remotely induced coherence can be used for entanglement detection, given the local energies or purities. A similar result has recently been obtained for extractable work with Gaussian measurements [43].

We mainly focus on two-mode states, but we also report an example of a feasible three-mode state, to explicitly show that Gaussian measurements on one mode induce both coherence and correlations in the remaining modes. Similar features have been investigated in finite-dimensional systems [16,18] and also generalized to arbitrary quantum operations beyond measurements [13].

A. General considerations for two-mode systems

At variance with the study of quantum correlations, the study of quantum coherence is highly influenced by local unitary operations. As a matter of fact, local displacement operations may increase the coherence of Gaussian states [21,22], and in turn, the first moments \mathbf{r} may play a role. On the other hand, in order to point out the role (and the interplay) of correlations and measurement back action in the generation of coherence, we assume vanishing first moments in the initial bipartite state. For the same reasons, we focus on the coherence of the most likely conditional state, i.e., according to the probability of outcomes in Eq. (8), the state with zero first moments. Indeed, the coherence gained by exploiting the

first moments cannot be linked to quantum correlations, since the first moments of a bipartite state can be controlled by local operations only. However, for completeness, in the Appendix we also extend the analysis by taking into account the effect of first moments.

We assume bipartite Gaussian states in normal form: states with zero mean $\mathbf{r}_A = \mathbf{r}_B = (0,0)$ and with the submatrices in Eq. (5) all diagonal and parametrized as $\sigma_A = a\mathbb{1}_2$, $\sigma_B = b\mathbb{1}_2$, and $\sigma_{AB} = \text{diag}(c_1, c_2)$. This choice is justified for two main reasons: (i) we want to focus on a class of bipartite states with incoherent (thermal) marginal states; and (ii) as previously explained for local displacement operations, also a local squeezing operation can indeed affect the coherence properties of the state, but it does not play any role as regards the correlations that are the main focus of this study.

Without loss of generality, we choose a Gaussian measurement represented by a diagonal covariance matrix $\sigma_m = \text{diag}(s, 1/s)$, i.e., squeezed along the x or p direction. Making these assumptions the conditional state has the CM and first moments

$$\sigma'_A = \begin{pmatrix} a - \frac{c_1^2}{b+s} & 0 \\ 0 & a - \frac{c_2^2}{b+s^{-1}} \end{pmatrix},$$

$$\mathbf{r}'_A = \begin{pmatrix} \frac{c_1}{b+s} & 0 \\ 0 & \frac{c_2}{b+s^{-1}} \end{pmatrix} \cdot \mathbf{r}_{\text{out}}; \quad (26)$$

as previously stated we focus on the case $\mathbf{r}_{\text{out}} = (0,0)$, which is the most likely outcome according to (8); this implies a conditional state with $\mathbf{r}'_A = (0,0)$.

B. Squeezed thermal states (STSs)

We first focus on two-mode squeezed thermal states, which means setting $c_1 = -c_2 = c$. We can get an intuition already by looking at the CM,

$$\begin{pmatrix} a - \frac{c^2}{b+s} & 0 \\ 0 & a - \frac{c^2}{b+s^{-1}} \end{pmatrix}; \quad (27)$$

we see that for heterodyne measurements ($s = 1$) we have a thermal state, which is incoherent, while the maximally squeezed state is obtained for homodyne measurements ($s \rightarrow \infty$).

For STS we focus on squeezing along the x direction since the direction of squeezing does not play a role, given the symmetry of the state. It can be useful to parametrize the measurement covariance matrix as $s = e^{2r_m}$ and $1/s = e^{-2r_m}$, where $r_m \geq 0$ is the ‘‘physical’’ squeezing parameter of the measurement; in the limit $r_m \rightarrow \infty$ ($s \rightarrow \infty$) we get a homodyne measurement of the quadrature \hat{p} .

It is interesting to note that conditional state (26) is insensitive to the sign of c_1 and c_2 . The same results are obtained for states with $c_1 = c_2 = c$, which will dub in the following mixed thermal states, which are always separable and physically correspond to thermal states mixed with a beam splitter. It follows that the same remote coherence can be created from these two classes of states for fixed a , b , and c , however, the range of physically allowed values of c is different in the two cases and STSs can be more correlated and, in fact, also entangled.

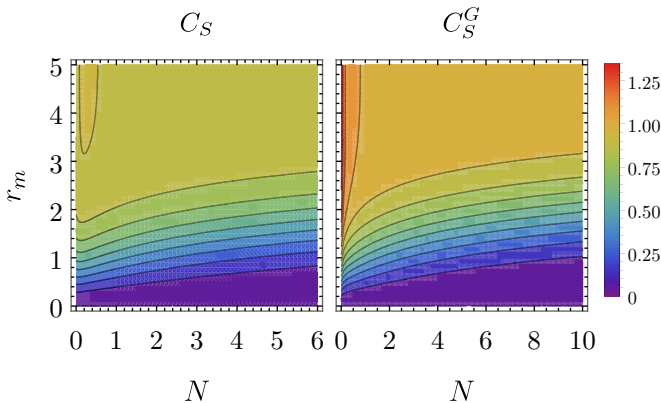


FIG. 1. Relative entropy of coherence C_S (left) and Gaussian relative entropy of coherence C_S^G (right) for the conditional state after Gaussian measurement of one mode of a symmetric STS. Coherence is shown as a function of the STS thermal photons N and the measurement squeezing r_m for a fixed value of the STS squeezing parameter $r = 1$.

In what follows we consider both the regular and the Gaussian relative entropy of coherence C_S and C_S^G . The measure C_S is computed numerically by truncating the Fock space and by evaluating the corresponding photon number distribution $\{\langle n|\rho|n\rangle\}$ needed to evaluate the Shannon entropy for generic single-mode Gaussian states [44,45].

1. Symmetric STSs

As a first step, we focus on symmetric STSs, for which local thermal states have the same energy, i.e., $a = b > 1$. The parameter c embodies the total correlations between the subsystems; for all these states, in order to satisfy the physicality condition, (4), one needs $|c| \leq \sqrt{a^2 - 1}$. We refer to the equality as the physicality threshold, which is achieved by pure STSs, i.e., the so-called *twin-beam* states. On the other hand, separable states must satisfy the condition $|c| \leq a - 1$, also referred to as the separability threshold, corresponding to the physicality threshold for symmetric STSs with the same parameter a . We also employ the physical parametrization of STSs: $a = b = (1 + 2N) \cosh 2r$ and $c_1 = -c_2 = (1 + 2N) \sinh 2r$, where $N \geq 0$ and $r \geq 0$ represent the number of thermal photons and a real squeezing parameter, respectively.

In Fig. 1 we show the behavior of the relative entropy of coherence C_S of the most probable conditional state and of its Gaussian version C_S^G as a function of the number of thermal photons N and the squeezing of the measurement r_m at fixed initial squeezing r . The behavior of both measures is similar: they both increase by increasing the squeezing of the measurement r_m and reach an asymptotic value for homodyne measurements ($r_m \rightarrow \infty$). They are both decreasing functions of the number of thermal photons N (at least for a sufficiently high N) and they tend to an asymptotic value dependent on r_m , as reported in [22]. The only relevant difference is that C_S initially shows a slight increment as a function of N . We also correctly show that C_S^G is an upper bound to C_S . These results indeed support the idea that by projecting subsystem B on a squeezed state we can generate coherence in subsystem A , even if the initial state is highly mixed. We have strong

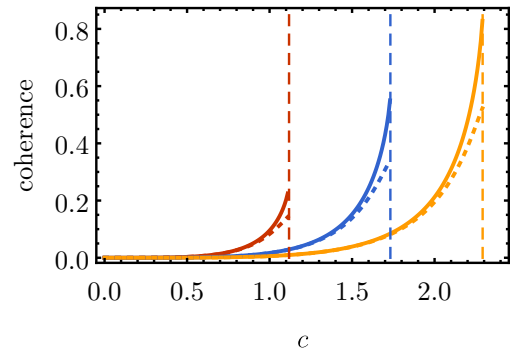


FIG. 2. Gaussian relative entropy of coherence C_S^G (upper, solid curves) and relative entropy of coherence C_S (lower, dotted lines) as a function of the covariance matrix term c for a symmetric STS and homodyne measurement ($s \rightarrow \infty$). From left to right the sets of curves represent $a = 1.5$ (red), $a = 2$ (blue), and $a = 2.5$ (yellow); vertical lines are drawn at the physicality bound $c = \sqrt{a^2 - 1}$.

numerical evidence that for this class of states the remote coherence is a monotonous function of the squeezing of the measurement r_m and, thus, that homodyne measurement is optimal. This is in agreement with physical intuition since a homodyne detection (with zero outcomes) amounts to a projection on an infinitely squeezed vacuum state and this kind of state becomes more and more coherent as far as the squeezing increases.

In Fig. 2 we show the maximal remote conditional coherence, obtained with a homodyne measurement, as a function of the parameter c , for different values of a , which also fixes the total energy of the state. We also have strong evidence that remote coherence is monotonically increasing in c at fixed a , i.e., by increasing the two-mode squeezing at a fixed energy.

Concerning the monotonicity (as a function of c and r_m) of the Gaussian measure C_S^G we can prove that the difference between the energy of the corresponding thermal state and the square root of the determinant of the covariance matrix [see Eq. (16)] is a monotonically increasing function. However, $h(x)$ being a concave function, this does not imply the monotonicity of C_S^G (but it is actually a condition implied by it). Overall, this suggests that our numerical result does indeed hold in general.

The monotonic behavior of remote coherence as a function of c implies that we can use this figure of merit for entanglement detection. Given the local energies $a = b$, there is a threshold value for the remote coherence which separates entangled and separable states. A very similar behavior was observed in [43] considering the extractable work via Gaussian measurements as a figure of merit. A similar bound on separable states also arises by considering quantum discord [46,47]; in that case, however, also an energy-independent bound exists. This feature is illustrated in Fig. 3, where one can see that the remote coherence for randomly generated symmetric STSs lie above the curve given at the separability threshold if and only if they are entangled, for both coherence measures.

2. Asymmetric STSs

We now consider asymmetric STSs, with two distinct local energies, $a > 1$ and $b > 1$. The physicality threshold

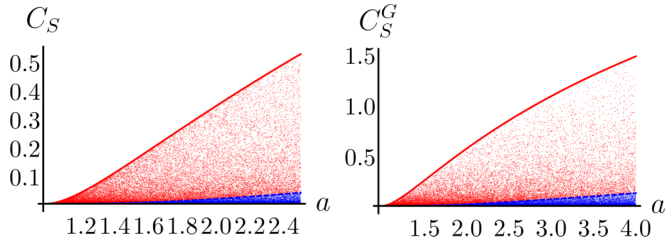


FIG. 3. Relative entropy of coherence (left) and Gaussian relative entropy of coherence (right) for homodyne measurement on mode B of a symmetric STS, as a function of a . The 5×10^4 random symmetric STSs are generated by sampling uniformly the parameters a and c . The solid red (dashed blue) curve at the top (in the middle) represents the physicality (separability) threshold. Entangled (separable) states correspond to red (blue) points above (below) the separability threshold.

is represented by the condition $|c| \leq \sqrt{ab - 1 - |a - b|}$, while the separability threshold is set by the condition $|c| \leq \sqrt{ab + 1 - a - b}$, which corresponds to the physicality threshold for asymmetric mixed thermal states with the same parameters.

Most of what we have learned for symmetric STSs still holds. We have numerical evidence that a homodyne measurement is optimal to remotely generate coherence and that remote coherence is a monotonically increasing function of c and of r_m at fixed a and b . This means that we have a bound on the remote coherence, which enables us to discriminate between separable and entangled states at fixed local energies, in complete analogy with the previous case. This is presented in Fig. 4, where we show that the remote coherence for randomly generated STSs lies above the surface at the separability threshold if and only if the states are entangled. The same results hold for both coherence monotones.

C. Generic states in normal form

We now consider the full class of standard-form two-mode states ($c_1 \neq \pm c_2$); the physicality and separability conditions are more involved and we do not report them explicitly (see [48] for a thorough analysis). We, again, have numerical evidence that homodyning is optimal for remote generation of coherence. However, a measurement of the quadrature x

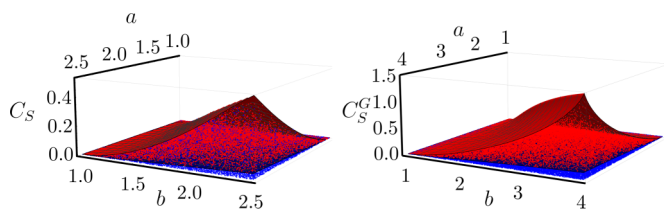


FIG. 4. Relative entropy of coherence (left) and Gaussian relative entropy of coherence (right) for homodyne measurements on mode B of asymmetric STSs, as a function of the parameters a and b . The 5×10^4 random asymmetric STSs are generated by sampling uniformly the parameters a , b , and c . The upper red (lower blue) surface corresponds to states on the physicality (separability) threshold. Entangled (separable) states correspond to red (blue) points above (below) the separability threshold.

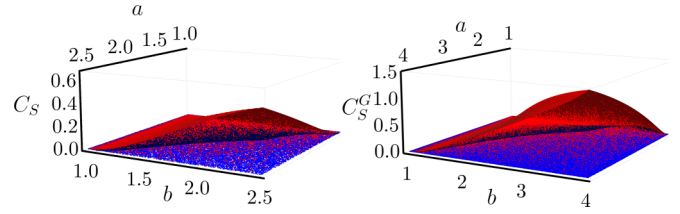


FIG. 5. Relative entropy of coherence (left) and Gaussian relative entropy of coherence (right) for optimal homodyne measurements on mode B of normal-form two-mode Gaussian states, as a function of the parameters a and b . The 5×10^4 (left) and 5×10^5 (right) random states in normal form are generated by sampling uniformly the parameters a , b , c_1 , and c_2 . The upper, red surface corresponds to states on the physicality threshold with maximal $|c_1|$, while the lower, blue surface corresponds to states on the physicality threshold with $c_2 = 0$. Entangled (separable) states correspond to lighter red (darker blue) points; only entangled states are above the lower, blue surface.

or p is optimal, depending on which canonical variables are more correlated, i.e., whether $|c_1| > |c_2|$ or the opposite. In the following we focus on the optimized remote coherence, generated by homodyning the appropriate quadrature.

The CM of the conditional state after homodyne measurements is a function of only one of the parameters c_1 and c_2 , depending on which quadrature is measured. The optimized remote coherence is thus a function of a single parameter, $c_{\max} = \max(|c_1|, |c_2|)$, and so the conjecture of monotonicity presented earlier still applies. At variance with STSs the entanglement of generic states in normal form is not a monotonic function of c_{\max} and one can find separable states with a greater c_{\max} than some entangled states. This implies that remote coherence cannot be used for discriminating entangled and separable states in this class, but we still have a conjectured bound at fixed local purities. We have numerical evidence that the upper value of c_{\max} for separable states (and therefore the maximal remote coherence) is obtained for the class of states with $c_2 = 0$ and $|c_1| = \sqrt{(a^2 - 1)(b^2 - 1)/(ab)}$, which are separable states at the physicality threshold. Obviously the roles of c_1 and c_2 could be exchanged.

In Fig. 5 we show the optimal remote coherence for random states in normal form; only entangled states lie above the surface given by separable states with maximal c_{\max} . The upper surface is obtained by numerically maximizing $|c_1|$ at the physicality threshold for a given a and b and coincides with pure STS states for $a = b$. These results also show that coherence due to measurement back action can be stronger for separable states than for entangled ones. This is somewhat similar to what happens in the task of remote state preparation, where discordant resource states can outperform entangled states [49]. However, in the present problem quantum discord is not a monotonic function of the remote coherence, therefore it cannot be regarded as a proper resource for the task.

D. Feasible three-mode state

In order to show that Gaussian measurements on a single mode can generate coherence and correlations in the bipartite conditional state we focus on a particular example: the pure tripartite obtained by interlinked bilinear interactions [50–52],

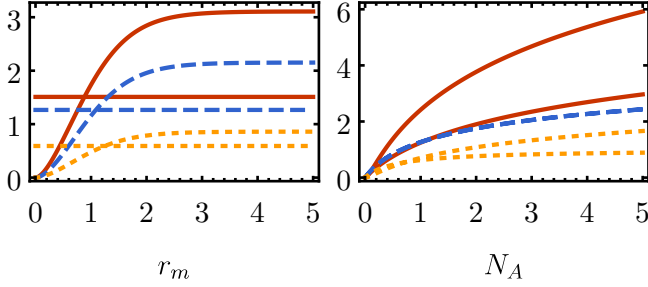


FIG. 6. Coherence and discord of the two-mode conditional state obtained by measuring mode A of the feasible three-mode state, (30). In both panels solid red curves represent C_S^G ; dashed blue curves, C_S ; and dotted orange curves, the quantum discord $D(B:C)$. In the left panel, the quantities are shown as a function of the measurement squeezing r_m at a fixed $N_B = 1$ and $N_C = 2$; horizontal lines correspond to the same figures of merit computed for the marginal state (and are thus independent of measurement squeezing). In the right panel, the quantities are shown as a function of N_A by fixing $N_B = N_C = N_A/2$, with $r_m = 5$; the lower curves correspond to the same figures of merit computed for the marginal state.

which is feasible experimentally. The first moments of this state are null, while its CM is

$$\Sigma_T = \begin{pmatrix} \sigma_A & \sigma_{AB} & \sigma_{AC} \\ \sigma_{AB} & \sigma_B & \sigma_{BC} \\ \sigma_{AC} & \sigma_{BC} & \sigma_C \end{pmatrix}, \quad (28)$$

where

$$\begin{aligned} \sigma_A &= (2N_A + 1)\mathbb{1}, & \sigma_B &= (2N_B + 1)\mathbb{1}, & \sigma_C &= (2N_C + 1)\mathbb{1}, \\ \sigma_{AB} &= 2\sqrt{N_B(N_A + 1)}\mathbb{P}, & \sigma_{AC} &= 2\sqrt{N_C(N_A + 1)}\mathbb{P}, \\ \sigma_{BC} &= 2\sqrt{N_B N_C}\mathbb{P}, \end{aligned} \quad (29)$$

with $N_A = N_B + N_C$ and $\mathbb{P} = \text{diag}(1, -1)$. The expansion on the Fock basis is the following:

$$\begin{aligned} |\xi\rangle &= \frac{1}{\sqrt{1 + N_A}} \sum_{p,q} \left(\frac{N_B}{1 + N_A} \right)^{p/2} \left(\frac{N_C}{1 + N_A} \right)^{q/2} \\ &\times \left[\frac{(p+q)!}{p!q!} \right]^{1/2} |p+q, p, q\rangle. \end{aligned} \quad (30)$$

We discuss the situation where a Gaussian measurement is performed on mode A and we study coherence and correlations of the conditional two-mode state of modes B and C . In this case, the marginal state is not locally thermal, but it is correlated and has quantum coherence.

In Fig. 6 we show the measurement-induced coherence, using both coherence measures, and the measurement-induced quantum discord, as a function of the total energy of the state and of the measurement squeezing. Since the conditional state remains pure, in this case quantum discord reduces to entanglement entropy. We also report the coherence and discord of the marginal state, explicitly showing that if measurement squeezing is not high enough, we obtain values lower than the ones we obtain by studying the initial marginal states. Furthermore, we correctly see that, as predicted by inequality (25), coherence of the two-mode state is always an upper bound to discord.

V. COHERENCE VIA CONTINUOUS GAUSSIAN MEASUREMENTS

We now consider a different protocol for producing single-mode coherence, based on continuous monitoring of the environmental degrees of freedom via Gaussian measurements. This setting bears some similarities to the protocol for remote creation of coherence considered in the previous section. In this case, the necessary correlations between the environment and the system are provided by the dynamics.

A. Gaussian conditional dynamics

We briefly review the notation and formalism needed to describe Gaussian conditional dynamics (see [26] for further details). We deal with a bosonic system in a Gaussian state, described by a covariance matrix σ and first moment vector \mathbf{r} . At each instant in time, the system interacts with a Markovian bath, described by input operators $\mathbf{r}_{\text{in}}(t)$ and correlation matrix σ_E , via a bilinear Hamiltonian,

$$\hat{H}_C = \hat{\mathbf{r}}^\top C \hat{\mathbf{r}}_{\text{in}}(t), \quad (31)$$

where C is an arbitrary matrix. If we trace out the degrees of freedom of the bath, i.e., we do not record measurements on the environmental degrees of freedom, the dynamics of the CM is described by a diffusion equation,

$$\dot{\sigma} = A\sigma + \sigma A^\top + D, \quad (32)$$

where

$$A = \Omega H_s + \frac{\Omega C \Omega C^\top}{2}, \quad D = \Omega C \sigma_E C^\top \Omega^\top. \quad (33)$$

If we also assume that the bath has zero first moments and that the system is not driven, the differential equation for the first moments then reads

$$\dot{\mathbf{r}}' = \mathbf{A}\mathbf{r}'. \quad (34)$$

Gaussian states are completely defined by first and second moments and thus one may derive the standard master equation in Lindblad form for the density operator from Eqs. (32) and (34).

If we introduce the continuous monitoring of the environmental modes through a Gaussian measurement described by a matrix σ_m , we find that the CM obeys a deterministic Riccati equation,

$$\dot{\sigma}' = \tilde{A}\sigma' + \sigma'\tilde{A}^\top + \tilde{D} - \sigma'BB^\top\sigma', \quad (35)$$

where we have defined

$$\tilde{A} = A - \Omega C \sigma_E (\sigma_E + \sigma_m)^{-1} \Omega C^\top, \quad (36)$$

$$\tilde{D} = D + \Omega C \sigma_E (\sigma_E + \sigma_m)^{-1} \sigma_E C^\top \Omega, \quad (37)$$

$$B = C \Omega (\sigma_E + \sigma_m)^{-\frac{1}{2}}; \quad (38)$$

as in the previous section, the CM σ_M defines a generic Gaussian measurement. On the contrary, the first moment's conditional evolution is stochastic and governed by

$$d\mathbf{r}' = \mathbf{A}\mathbf{r}'dt + (\Omega C \sigma_E - \sigma' C \Omega) (\sigma_E + \sigma_m)^{\frac{1}{2}} \frac{d\mathbf{w}}{\sqrt{2}}, \quad (39)$$

which is an Ito stochastic differential equation corresponding to a classical Wiener process; the vector of Wiener increments $d\mathbf{w}$ satisfies $dw_j^2 = dt$.

B. Coherence of a monitored quantum optical parametric oscillator

We now focus on the simple model of a single-mode quantum optical parametric oscillator, physically composed by an optical cavity mode driven by a pump laser and interacting with a nonlinear optical crystal. The effective Hamiltonian for the system is

$$H_s = -\frac{\chi}{2}(\hat{x}\hat{p} + \hat{p}\hat{x}), \quad (40)$$

where \hat{x} and \hat{p} are conjugated quadratures of the field being amplified and χ is a coupling constant given by the second-order nonlinear coefficient of the crystal times the average photon number of the pump laser. We consider the system interacting with a Markovian bath at thermal equilibrium, which can be described by a single-mode CM of the form

$$\sigma_E = \frac{1}{\mu} \mathbb{1}_2 \quad \mu = (2N + 1)^{-1}. \quad (41)$$

The interaction between the cavity mode and the environment is passive and modeled by the Hamiltonian

$$H_C = \sqrt{\gamma}(\hat{x}\hat{x}_{in}(t) + \hat{p}\hat{p}_{in}(t)), \quad (42)$$

such that the coupling matrix reads $C = \sqrt{\gamma}\mathbb{1}_2$. If the environment is left unmonitored, then the unconditional dynamics is described by the standard quantum optical master equation. The unconditional dynamics is stable and admits a steady state for $\chi < \frac{\gamma}{2}$; the steady-state CM is found by imposing $\dot{\sigma} = 0$ in Eq. (32) and reads

$$\sigma_{ss} = \frac{1}{\mu} \begin{pmatrix} \frac{1}{1+2\tilde{\chi}} & 0 \\ 0 & \frac{1}{1-2\tilde{\chi}} \end{pmatrix}; \quad (43)$$

while the first moments are null, for convenience we have defined $\tilde{\chi} = \frac{\chi}{\gamma}$, so that the stability condition becomes $\tilde{\chi} \leq \frac{1}{2}$.

The steady state is clearly squeezed and thus has nonzero quantum coherence. We now show that its quantum coherence can be improved, thanks to environmental monitoring, if the measurements are projections on states which are squeezed enough. For general-dyne monitoring with unit efficiency and real squeezing parameter, i.e., a pure and diagonal σ_m as defined in the previous section, matrices (36) become

$$\tilde{A} = \begin{pmatrix} -\chi - \frac{1}{2} \frac{\gamma\mu e^{-2r_m}}{1+\mu e^{-2r_m}} & 0 \\ 0 & \chi - \frac{1}{2} \frac{\gamma\mu e^{2r_m}}{1+\mu e^{2r_m}} \end{pmatrix}, \quad (44)$$

$$\tilde{D} = \frac{\gamma}{\mu} \begin{pmatrix} \frac{\mu e^{-2r_m}}{1+\mu e^{-2r_m}} & 0 \\ 0 & \frac{\mu e^{2r_m}}{1+\mu e^{2r_m}} \end{pmatrix}, \quad (45)$$

$$B = \sqrt{\mu\gamma} \begin{pmatrix} 0 & \sqrt{\frac{1}{1+\mu e^{-2r_m}}} \\ -\sqrt{\frac{1}{1+\mu e^{2r_m}}} & 0 \end{pmatrix}. \quad (46)$$

The steady-state CM of the conditional dynamics is obtained by setting $\dot{\sigma} = 0$ in Eq. (35); the result of the algebraic equation

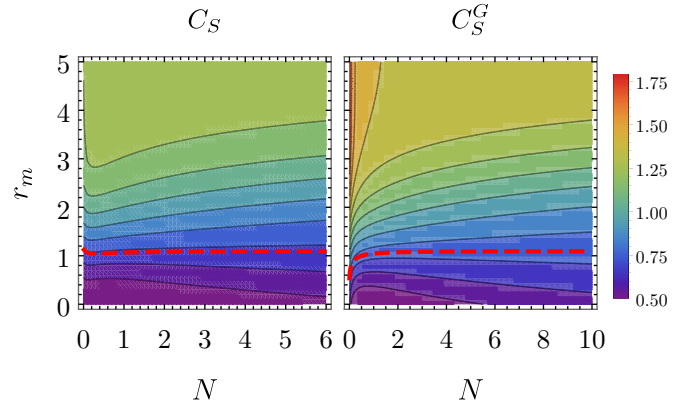


FIG. 7. Steady-state coherence (at zero first moments). In the left panel we have the relative entropy of coherence and in the right panel its Gaussian counterpart, both as a function of the measurement squeezing r_m and the mean number of excitations of the environmental mode N , with fixed $\tilde{\chi} = 0.4$. Dashed red lines represent the threshold values r_m^{th} for which the coherence of the monitored state is equal to that of the unconditional dynamics. In the region above the red curve we have more coherence than for unconditional dynamics; in the region below the curve, vice versa.

is

$$\sigma'_{ss} = \begin{pmatrix} \frac{\tilde{A}_{11} + \sqrt{\tilde{A}_{11}^2 + (BB^\tau)_{11}\tilde{D}_{11}}}{(BB^\tau)_{11}} & 0 \\ 0 & \frac{\tilde{A}_{22} + \sqrt{\tilde{A}_{22}^2 + (BB^\tau)_{22}\tilde{D}_{22}}}{(BB^\tau)_{22}} \end{pmatrix}, \quad (47)$$

which, again, is a function of the parameter $\tilde{\chi}$. For homodyne detection of \hat{p} ($r_m \rightarrow \infty$) we obtain a thermal squeezed state with exactly N thermal photons and a squeezing parameter dependent on $\tilde{\chi}$, described by the CM

$$\sigma_{ss}^{(\text{hom})} = \frac{1}{\mu} \begin{pmatrix} 1 - 2\tilde{\chi} & 0 \\ 0 & \frac{1}{1-2\tilde{\chi}} \end{pmatrix}. \quad (48)$$

This scenario is similar to the one we have studied in the previous sections. Also in this case, we neglect the first moments of the steady state. Indeed, the zero-first-moments case corresponds to the most likely event. In addition, the coherence achievable by nonzero first moments may be achieved by displacing the state afterward as well.

In Fig. 7 we show both measures of coherence for the monitored steady state as a function of the mean thermal excitations N of the environmental state and of the measurement squeezing r_m . We find again that, neglecting first moments, the best possible measurement is homodyne detection, whereas a certain amount of squeezing is needed to surpass the coherence of the unmonitored state.

In Fig. 8 we show the threshold value of the measurement squeezing r_m^{th} for which the coherence of the monitored state is equal to that of the unconditional dynamics (always neglecting first moments). We see that it is an increasing function of $\tilde{\chi}$; as a matter of fact, for $\tilde{\chi} \rightarrow \infty$ the unconditional state becomes more and more squeezed, therefore a homodyne measurement is needed to achieve the same coherence in the conditional state. In general, the two coherence monotones produce different threshold values, but this is noticeable only in the low- N regime, and for larger N the curves are

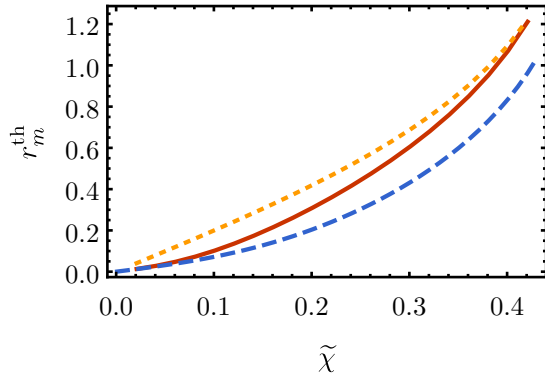


FIG. 8. Value of the threshold squeezing as a function of $\tilde{\chi}$. The solid red curve is obtained for C_S , and the dashed blue for C_S^G , both for $N = 0.1$; the dotted yellow curve represents both C_S and C_S^G for $N = 5$.

indistinguishable. Moreover, in Fig. 7 we also show r_m^{th} as a function of N for a particular fixed value of $\tilde{\chi}$ and we see that it quickly saturates to an asymptotic value for growing N .

VI. CONCLUSIONS

In this paper, we have addressed the measurement-based generation of quantum coherence in continuous variable systems and investigated the coherence induced by Gaussian measurements on correlated Gaussian systems. We have first explored a scenario for remote creation of coherence and analyzed in some detail the interplay with classical and quantum correlations. Starting from bipartite squeezed thermal states the remote coherence created by Gaussian measurements is a monotonic function of the relevant off-diagonal term of the covariance matrix, which in turn expresses the correlations among the canonical observables of the two parties. Given the symmetry of STSs, also entanglement and discord are monotonic functions of the same parameter. As a consequence, conditional coherence induced by measurement may be used to discriminate between entangled and separable states, given the local purities. This is no longer true for the case of a generic two-mode state in normal form, for which we found a sufficient condition for detecting entangled states. A key finding is that measurement-induced coherence is not directly linked to quantum correlations but, rather, to classical correlations between the two parties.

We have also evaluated the conditional coherence achievable by conditional measurements on a specific class of three-mode states which are experimental feasible. From this we highlight that measurement on a single mode induces both coherence and quantum correlations in the remaining two-mode system. In particular, we have shown that two-mode coherence on the Fock basis is an upper bound to the quantum discord.

We then explored the coherence achievable by the continuous monitoring of the environment of a continuous variable system. In particular, we have discussed the dynamics of an optical parametric oscillator and investigated how the coherence may be increased by means of time-continuous Gaussian measurement on the interacting environment. In this

case, we found that also the unconditional state has nonzero coherence, but there exists a threshold on the measurement squeezing above which coherence is enhanced by the conditional measurement.

Overall, our results show that Gaussian measurements represent a resource to create conditional coherence, which in turn may be exploited as an entanglement witness.

ACKNOWLEDGMENT

This work was supported by the E.U. through the projects QuProCS (Grant Agreement No. 641277) and ConAQuMe (Grant Agreement No. 701154).

APPENDIX: NONZERO OUTCOMES AND AVERAGE COHERENCE

In this Appendix, we relax the assumption of zero measurement outcomes. We explore the effect of first moments on the remote creation of coherence and we also look at the average coherence with regard to the probability distribution of the outcomes. For simplicity, we restrict the analysis to two-mode STSs.

1. First moments of the conditional state

Let us consider a two-mode STS with covariance matrix σ and a general-dyne measurement, characterized by the CM of a pure single-mode state:

$$\begin{aligned} \sigma_m &= R(\phi) \begin{pmatrix} s & 0 \\ 0 & 1/s \end{pmatrix} R(\phi)^\top \\ &= \begin{pmatrix} s \cos^2 \phi + \frac{\sin^2 \phi}{s} & \frac{(s^2-1) \cos \phi \sin \phi}{s} \\ \frac{(s^2-1) \cos \phi \sin \phi}{s} & \frac{\cos^2 \phi}{s} + s \sin^2 \phi \end{pmatrix}; \end{aligned} \quad (\text{A1})$$

the covariance matrix σ'_A and first moments \mathbf{r}'_A of the conditional state in mode A after the measurement σ_m is performed on mode B are given by Eqs. (7). We now want to explicitly evaluate the mean number of excitations due to the first moment of this state, i.e., $\frac{1}{2}|\mathbf{r}'_A|^2$, as the Gaussian measure of coherence, (16), monotonously depends on it. We write the outcome of the measurement in polar coordinates $\mathbf{r}_{\text{out}} = (|\mathbf{r}_{\text{out}}| \cos \theta, |\mathbf{r}_{\text{out}}| \sin \theta)$ and evaluate the term depending on the first moments explicitly:

$$\begin{aligned} |\mathbf{r}'_A|^2 &= \frac{c^2 |\mathbf{r}_{\text{out}}|^2 s}{(b+s)(bs+1)} \left\{ (b^2-1) \right. \\ &\quad \left. + \left(2b+s+\frac{1}{s} \right) \left[s \sin^2(\theta-\phi) + \frac{\cos^2(\theta-\phi)}{s} \right] \right\}. \end{aligned} \quad (\text{A2})$$

As is apparent from the above formula, the relevant parameter is the relative angle $\phi - \theta$ between the squeezing and the measurement outcome vector. Without loss of generality we can choose $s \geq 1$; in this case the energy is maximized by $\phi - \theta = (k + 1/2)\pi$, with $k \in \mathbb{Z}$.

For heterodyne measurement ($s = 1$) the dependence on the angles is suppressed, resulting in

$$|\mathbf{r}'_A^{(\text{het})}|^2 = \frac{c^2 |\mathbf{r}_{\text{out}}|^2}{(b+1)^2}, \quad (\text{A3})$$

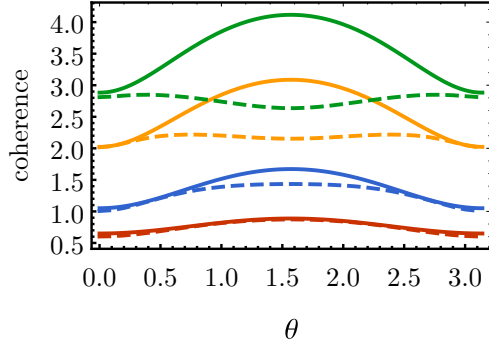


FIG. 9. Remote coherence as a function of the outcome angle θ for a symmetric STS with $N = 1$ and $r = 1$. From bottom to top we have $|\mathbf{r}_{\text{out}}| = 1$ (red lines), $|\mathbf{r}_{\text{out}}| = 2$ (blue lines), $|\mathbf{r}_{\text{out}}| = 4$ (yellow lines), and $|\mathbf{r}_{\text{out}}| = 6$ (green lines). Dashed lines represent the relative entropy of coherence C_S ; solid lines, the Gaussian counterpart C_S^G .

while in the homodyne limit $s \rightarrow \infty$ we have

$$|\mathbf{r}_A^{(\text{hom})}|^2 = \frac{c^2 |\mathbf{r}_{\text{out}}|^2 \sin^2(\theta - \phi)}{b^2}. \quad (\text{A4})$$

2. Remote coherence for nonzero outcomes

A nonzero measurement outcome $|\mathbf{r}_{\text{out}}| \neq 0$ implies a nonzero first moments vector \mathbf{r}'_A of the conditional state, which in turn means a higher coherence than in the zero-outcome case. This is evident in Eq. (16) for the Gaussian relative entropy of coherence, but it is true also for the relative entropy of coherence. As shown in the previous section, the quantity $|\mathbf{r}'_A|^2$ depends on the angle $\phi - \theta$. In particular, if we fix the measurement angle $\phi = 0$ the maximum is for $\theta = \frac{\pi}{2}$, i.e., when the outcome vector is displaced along the p axis. The same behavior is shared by the Gaussian measure of coherence, which is maximal for $\theta = \frac{\pi}{2}$ at fixed $|\mathbf{r}_{\text{out}}|$. This is shown in Fig. 9, where we also show that the behavior of the relative entropy of coherence is different in general.

In Fig. 10 we show the remote coherence as a function of $r_m = \frac{1}{2} \log_2 s$ for $\phi = 0$ (as $r_m \rightarrow \infty$ it becomes a measurement of \hat{p}) for different values of the outcome vector \mathbf{r}_{out} .

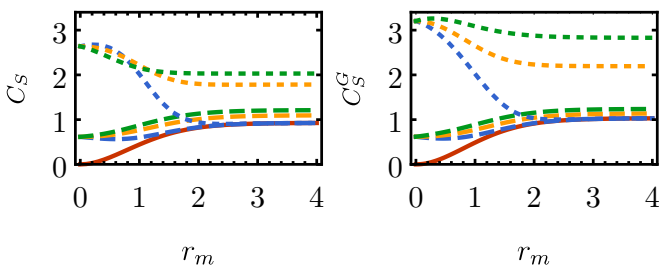


FIG. 10. Relative entropy of coherence (top) and Gaussian relative entropy of coherence (bottom) as a function of r_m for a symmetric STS with $N = 1$ and $r = 1$. The lowest, solid red curve is for zero outcome, $|\mathbf{r}_{\text{out}}| = 0$. The blue, yellow, and green dashed curves in the middle represent $|\mathbf{r}_{\text{out}}| = 1$ and $\theta = 0, \frac{\pi}{4}$, and $\frac{\pi}{2}$ (from bottom to top), respectively. The blue, yellow, and green dotted curves at the top are for $|\mathbf{r}_{\text{out}}| = 4$ and $\theta = 0, \frac{\pi}{4}$, and $\frac{\pi}{2}$ (from bottom to top in the region $r_m \approx 2$), respectively.

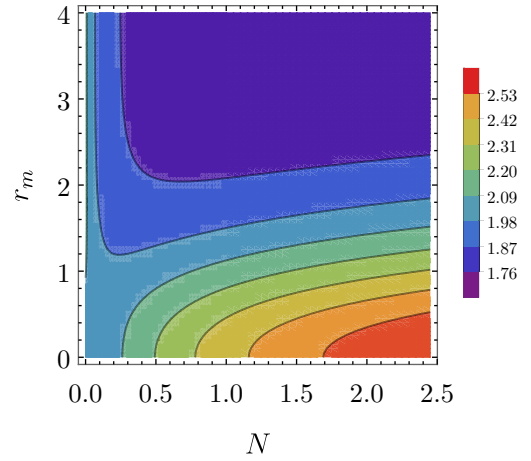


FIG. 11. The average remote Gaussian relative entropy of coherence \bar{C}_S^G for fixed $r = 1$ as a function of r_m and N .

At variance with the case studied in the text, measurement squeezing can actually decrease the amount of coherence obtainable, depending on the value of the outcome vector. Moreover, we can see again the different behavior of the two coherence measures, evident in the curves obtained for $|\mathbf{r}_{\text{out}}| = 4$. These considerations resemble one of the results in [13], where the coherence generated by selective measurements is upper bounded by a term inversely proportional to the probability of getting the final state (calculation carried out for finite dimensions using the l_1 norm of coherence). In a similar way, in our Gaussian scenario the greater $|\mathbf{r}_{\text{out}}|$ is, the smaller the value of the probability density $p(\mathbf{r}_{\text{out}})$. For fixed $|\mathbf{r}_{\text{out}}|$ and $\phi = 0$, the more displaced the state in the p direction, the lower the value of the probability of getting that state. This happens because a Gaussian measurement with $\phi = 0$ and $s > 1$ has a Gaussian distribution of the outcomes $p(\mathbf{r}_{\text{out}})$ which is “squeezed” along the x axis.

3. Average remote coherence

By dropping the zero-outcome assumption, the most interesting quantity to consider is the average coherence that

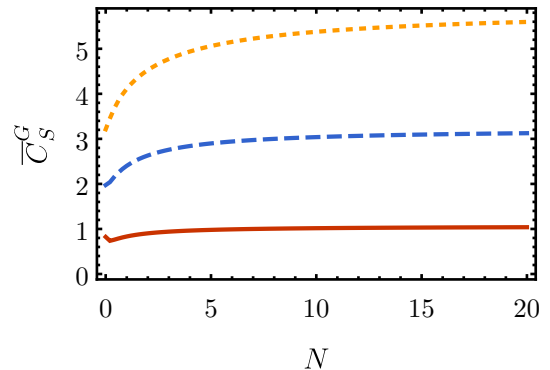


FIG. 12. The average remote Gaussian relative entropy of coherence \bar{C}_S^G for heterodyne measurements ($r_m = 0$) and a symmetrical STS as a function of N . Different curves represent different values of the initial squeezing: $r = 0.5$ (solid red line), $r = 1$ (dashed blue line), and $r = 1.5$ (dotted yellow line).

can be harvested if nonselective measurements are made on subsystem B and all possible results are recorded. This figure of merit has been studied at length [13,16]. Given a coherence measure $C(\rho)$, in our continuous variable setting it is defined as

$$\bar{C}^{A|B} = \int d^2\mathbf{r}_{\text{out}} p(\mathbf{r}_{\text{out}}) C(\rho'_A), \quad (\text{A5})$$

where $p(\mathbf{r}_{\text{out}})$ is the Gaussian distribution given by Eq. (8); in the following, we omit the superscript $A|B$, because we always consider measurements on subsystem B and we are interested in the coherence of system A . In order to compute \bar{C}_S^G the integral has to be evaluated numerically; computing \bar{C}_S is trickier because there is no closed formula for C_S in the Gaussian case. The contour plot of the average Gaussian relative entropy of coherence as a

function of N and r_m for a symmetrical STS is shown in Fig. 11.

We see that a heterodyne measurements yields the best average remote Gaussian coherence, at variance with the case of null outcomes. Moreover, the average Gaussian coherence actually increases with more mixed initial states, i.e., increasing N . This fact is explicitly shown in Fig. 12, where we report the results for heterodyne measurements as a function of N and we see that the average coherence tends to an asymptotic value.

The analogous figure of merit in the continuous measurement setup in Sec. V would be the average coherence with regard to the stationary probability distribution of the first moments. This probability distribution is the stationary solution of the Fokker-Planck equation associated with the Wiener process in Eq. (39).

-
- [1] R. J. Glauber, *Phys. Rev.* **130**, 2529 (1963).
 [2] L. Mandel and E. Wolf, *Rev. Mod. Phys.* **37**, 231 (1965).
 [3] A. Albrecht, *J. Mod. Opt.* **41**, 2467 (1994).
 [4] M. Hillery, *Phys. Rev. A* **93**, 012111 (2016).
 [5] H.-L. Shi, S.-Y. Liu, X.-H. Wang, W.-L. Yang, Z.-Y. Yang, and H. Fan, *Phys. Rev. A* **95**, 032307 (2017).
 [6] M. Lostaglio, D. Jennings, and T. Rudolph, *Nat. Commun.* **6**, 6383 (2015).
 [7] K. Korzekwa, M. Lostaglio, J. Oppenheim, and D. Jennings, *New J. Phys.* **18**, 023045 (2016).
 [8] P. Giorda and M. Allegra, [arXiv:1611.02519](https://arxiv.org/abs/1611.02519).
 [9] S. F. Huelga and M. B. Plenio, *Contemp. Phys.* **54**, 181 (2013).
 [10] T. Baumgratz, M. Cramer, and M. B. Plenio, *Phys. Rev. Lett.* **113**, 140401 (2014).
 [11] A. Streltsov, G. Adesso, and M. B. Plenio, [arXiv:1609.02439](https://arxiv.org/abs/1609.02439).
 [12] J. Ma, B. Yadin, D. Girolami, V. Vedral, and M. Gu, *Phys. Rev. Lett.* **116**, 160407 (2016).
 [13] T. Ma, M.-J. Zhao, S.-M. Fei, and G.-L. Long, *Phys. Rev. A* **94**, 042312 (2016).
 [14] E. Chitambar, A. Streltsov, S. Rana, M. N. Bera, G. Adesso, and M. Lewenstein, *Phys. Rev. Lett.* **116**, 070402 (2016).
 [15] K.-D. Wu, Z. Hou, H.-S. Zhong, Y. Yuan, G.-Y. Xiang, C.-F. Li, and G.-C. Guo, [arXiv:1702.06606](https://arxiv.org/abs/1702.06606).
 [16] X. Hu and H. Fan, *Sci. Rep.* **6**, 34380 (2016).
 [17] M.-L. Hu, X. Hu, J.-C. Wang, Y. Peng, Y.-R. Zhang, and H. Fan, [arXiv:1703.01852](https://arxiv.org/abs/1703.01852).
 [18] J. Zhang, S.-R. Yang, Y. Zhang, and C.-s. Yu, [arXiv:1703.02737](https://arxiv.org/abs/1703.02737).
 [19] X.-L. Wang, Q.-L. Yue, C.-H. Yu, F. Gao, and S.-J. Qin, [arXiv:1703.00648](https://arxiv.org/abs/1703.00648).
 [20] Y.-R. Zhang, L.-H. Shao, Y. Li, and H. Fan, *Phys. Rev. A* **93**, 012334 (2016).
 [21] J. Xu, *Phys. Rev. A* **93**, 032111 (2016).
 [22] D. Buono, G. Nocerino, G. Petrillo, G. Torre, G. Zonzo, and F. Illuminati, [arXiv:1609.00913](https://arxiv.org/abs/1609.00913).
 [23] C. Gehrke, J. Sperling, and W. Vogel, *Phys. Rev. A* **86**, 052118 (2012).
 [24] S. Ryl, J. Sperling, and W. Vogel, *Phys. Rev. A* **95**, 053825 (2017).
 [25] K. C. Tan, T. Volkoff, H. Kwon, and H. Jeong, [arXiv:1703.01067](https://arxiv.org/abs/1703.01067).
 [26] M. G. Genoni, L. Lami, and A. Serafini, *Contemp. Phys.* **57**, 331 (2016).
 [27] R. Simon, N. Mukunda, and B. Dutta, *Phys. Rev. A* **49**, 1567 (1994).
 [28] R. Simon, *Phys. Rev. Lett.* **84**, 2726 (2000).
 [29] R. Blandino, M. G. Genoni, J. Etesse, M. Barbieri, M. G. A. Paris, P. Grangier, and R. Tualle-Brouri, *Phys. Rev. Lett.* **109**, 180402 (2012).
 [30] E. Chitambar and G. Gour, *Phys. Rev. Lett.* **117**, 030401 (2016).
 [31] E. Chitambar and G. Gour, *Phys. Rev. A* **94**, 052336 (2016).
 [32] I. Marvian and R. W. Spekkens, *Phys. Rev. A* **94**, 052324 (2016).
 [33] X.-D. Yu, D.-J. Zhang, G. F. Xu, and D. M. Tong, *Phys. Rev. A* **94**, 060302(R) (2016).
 [34] M. G. Genoni, M. G. A. Paris, and K. Banaszek, *Phys. Rev. A* **78**, 060303(R) (2008).
 [35] M. G. Genoni and M. G. A. Paris, *Phys. Rev. A* **82**, 052341 (2010).
 [36] Z. Xi, Y. Li, and H. Fan, *Sci. Rep.* **5**, 10922 (2015).
 [37] Y. Yao, X. Xiao, L. Ge, and C. P. Sun, *Phys. Rev. A* **92**, 022112 (2015).
 [38] K. C. Tan, H. Kwon, C.-Y. Park, and H. Jeong, *Phys. Rev. A* **94**, 022329 (2016).
 [39] Y. Guo and S. Goswami, *Phys. Rev. A* **95**, 062340 (2017).
 [40] S. Luo, *Phys. Rev. A* **77**, 022301 (2008).
 [41] L. Mišta, Jr., R. Tatham, D. Girolami, N. Korolkova, and G. Adesso, *Phys. Rev. A* **83**, 042325 (2011).
 [42] Q. Zheng, J. Xu, Y. Yao, and Y. Li, *Phys. Rev. A* **94**, 052314 (2016).
 [43] M. Brunelli, M. G. Genoni, M. Barbieri, and M. Paternostro, [arXiv:1702.05110](https://arxiv.org/abs/1702.05110).
 [44] P. Marian and T. A. Marian, *Phys. Rev. A* **47**, 4474 (1993).
 [45] V. V. Dodonov, O. V. Man'ko, and V. I. Man'ko, *Phys. Rev. A* **49**, 2993 (1994).
 [46] G. Adesso and A. Datta, *Phys. Rev. Lett.* **105**, 030501 (2010).
 [47] P. Giorda and M. G. A. Paris, *Phys. Rev. Lett.* **105**, 020503 (2010).
 [48] S. Pirandola, A. Serafini, and S. Lloyd, *Phys. Rev. A* **79**, 052327 (2009).

- [49] B. Dakić, Y. O. Lipp, X. Ma, M. Ringbauer, S. Kropatschek, S. Barz, T. Paterek, V. Vedral, A. Zeilinger, Č. Brukner, and P. Walther, *Nat. Phys.* **8**, 666 (2012).
- [50] R. A. Andrews, H. Rabin, and C. L. Tang, *Phys. Rev. Lett.* **25**, 605 (1970).
- [51] A. Ferraro, M. G. A. Paris, M. Bondani, A. Allevi, E. Puddu, and A. Andreoni, *J. Opt. Soc. Am. B* **21**, 1241 (2004).
- [52] S. Olivares and M. G. A. Paris, *Int. J. Mod. Phys. B* **27**, 1345024 (2013).